LANGMUIR

pubs.acs.org/Langmuir Article

Rapid Growth of Colloidal Crystal Films from the Concentrated Aqueous Ethanol Suspension

Giang T.H. Tran, Masaki Koike, Tetsuo Uchikoshi, and Hiroshi Fudouzi*

Cite This: *Langmuir* 2020, 36, 10683−10689 Read Online

ACCESS | Metrics & More | Article Recommendations | Supporting Information

ABSTRACT: Developing a rapid fabrication of colloidal crystal film is one of the technical issues to apply to wide and various fields. We have been investigating a drying process of colloidal aqueous ethanol (EtOH) suspension formed by electrophoretic deposition (EPD). Here, the detailed formation mechanism of the colloidal crystal films with the closest packing structure was investigated by optical microscope and spectroscopy. The growth mechanism from the colloidal suspension to the colloidal crystal film was found to consist of four stages. In the first stage, concentrated colloidal suspension changed to order structure, i.e., nonclosely packed colloidal crystal by Alder phase transition. After this crystallization, we observed Bragg's diffraction peak and structural color. In the second stage, the diffraction peak shifts toward the shorter-wavelength direction (blue shift) due to the reduction of the interparticle distance of the nonclosely packed colloidal crystal. Finally, this peak shift continued until the closely packed colloidal crystal film was formed. In the third stage, the diffraction peak kept almost a similar wavelength due to the liquid film of aqueous EtOH covering on the colloidal crystal film. In the fourth stage, the colloidal crystal film changed from wet to dry condition. The structural color changes from green to blue by the evaporation of the solvent from the interspace of the colloidal crystal film. This color change is explained by the change in the refractive index of the interparticle medium from solvent to air. One of the key findings in our process is a rapid crystal growth using concentrated colloid aqueous EtOH suspension. Drying the concentrated suspension formed a closely packed colloidal crystal film within 55 s. This process has the potential for high-speed deposition of the colloidal crystalline thin films.

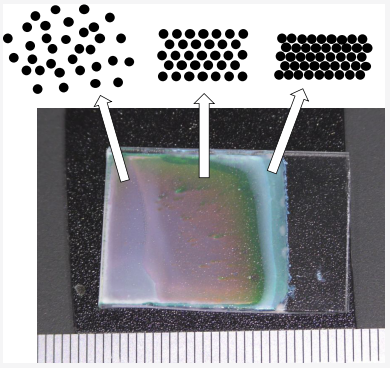

INTRODUCTION

Interest in colloidal crystal films as two-dimensional/three-dimensional (2D/3D) photonic materials and structural color substances has been continuously increasing due to the extending applications, such as photonic ink systems, photonic rubber sheet and crystal lasers, bio/chemical sensors, and bioinspired materials.[1−8] These types of films, i.e., colloidal crystal films, have been synthesized by the various techniques, such as solvent evaporation,[9,10] template-directed crystallization,[11] natural sedimentation,[12] vertical deposition methods,[13,14] cell packing method,[15] oil covering method,[16] floating packings,[17] electric-field-assisted convective assembly,[18] and air-pulse-drive assembly.[19] An electrophoretic deposition (EPD) technique has been getting attention recently to potentially realize the fast fabrication of colloidal crystal films.

Rogach et al. reported the colloidal crystal film formation within 30 min by the EPD process.[20] Since then, this process was considered to be advantageous for the rapid formation of the colloidal crystal structure. Several groups reported the colloidal crystal film formation by the EPD process with dimensions of about 1−5 cm^2 during 30−120 min.[21,22] Shape-controlled fabrication such as cylindrical form colloidal crystal film was also demonstrated.[23] We have been investigating the EPD process in detail to realize the rapid colloidal crystal film fabrication.[24,25] The mixture of water and ethanol (EtOH) with high EtOH concentration was found as a proper suspension. To optimize the EPD colloidal crystal film formation process, a multiple-step mechanism was applied. Although the EPD process is characterized by the migration of colloidal particles in a liquid under an electric field and the subsequent deposition, we have recently found that the colloidal crystal film formation did not take place by the EPD process itself. It seems that the colloidal crystal film formation took place during the following drying up process.

In another sense, a colloidal crystal film formation mechanism has not been understood well in the previous EPD process. In the drying step in our EPD experiment, we have observed the color change from milky white to green within a few minutes. Similar phenomena were reported in previous papers on the colloidal crystal film formation. The color change was observed at the crystallization process and the peak shift of Bragg's diffraction was investigated.[16,26−31] In this paper, the detailed

Received: April 20, 2020
Revised: August 17, 2020
Published: August 20, 2020

https://dx.doi.org/10.1021/acs.langmuir.0c01048
Langmuir 2020, 36, 10683−10689

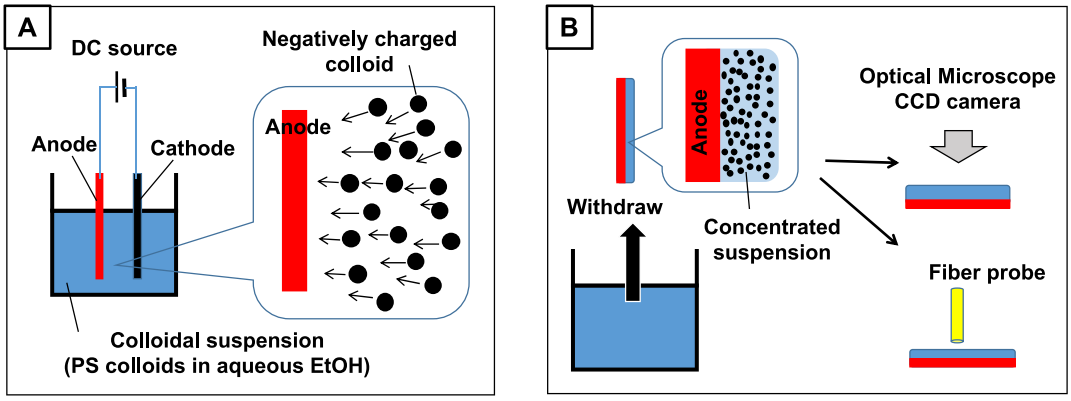

Figure 1. Experimental procedure of electrophoresis and drying process. (A) Negatively charged PS colloids migrated to anode substrate. (B) Drying process after withdrawing from colloidal suspension and observation and measurement for the formation of colloidal crystal film.

mechanism to form a colloidal crystal structure from the concentrated aqueous EtOH suspension in the drying process will be elucidated.

EXPERIMENTAL SECTION

Chemicals and Materials. Polystyrene (PS) colloids were synthesized by the standard emulsion polymerization method. PS colloids were monodispersed in the water at 7.54 wt %. The average diameter of the PS colloid was 204.2 nm, measured by a scanning electron microscope image. For the EPD experiment, the aqueous PS colloidal suspension was mixed with ethanol (99.5%, Kanto Chemical Co., Inc.) at 1:4 weight ratio based on our previous work.[24,25] As a result, the mixed solvent was 81.7 vol % EtOH. An indium tin oxide (ITO) coated glass as the anode electrode was obtained from Geomatec Co., Ltd. A stainless steel (SUS304) plate as the cathode electrode was obtained from the NILACO Corporation.

EPD Procedure. Colloidal crystal films were formed on ITO glass substrates by electrophoresis deposition. Figure 1 shows the schematic of the electrophoresis and drying process. Figure 1A is a setup layout of electrophoresis in PS colloidal suspension. An ITO/glass plate cut in the dimensions of 20 mm × 30 mm was used as an anodic substrate. A stainless steel plate with the same size was used as a counter electrode/cathode. The distance from the ITO/glass to a stainless steel plate was 1.0 cm. After immersing the electrodes in the colloidal suspension, 5 V/cm DC voltage was applied for 5 min.

As shown in the insert illustration of Figure 1A, where PS colloid particles migrate to the anodic substrate since PS colloids are negatively charged in the suspension. After the EPD process, the substrate was pulled out from the suspension, as shown in Figure 1B. The surface of the anode substrate was covered with concentrated PS colloidal suspension liquid film. The liquid film shows a white milky color and no structural color, i.e., colloidal PS particles are randomly arranged in the suspension. The optimum withdrawing speed was set at 3 mm/s.[25] The change in the suspension during drying evolution was observed by a CCD camera with an optical microscope at room temperature. In addition, the colloidal crystallization was measured by reflectance spectroscopy with a fiber probe, as shown in Figure 1B.

Characterization. The drying processes were observed with a digital 4K video camera (HC-VX985M, PANASONIC). Changes in the microstructure during the drying process were observed with an optical microscope (OptiPhoto II, NIKON) mounted with a CMOS camera (TrueChrome HD, TUCSEN). The microstructure of colloidal crystal films was observed by a scanning electron microscope (JSM-6500F, JEOL). Local reflection spectra were measured by a miniature fiber-optic spectrometer (USB2000, OCEAN INSIGHT) with a reflection fiber probe (R200-7-UV−VIS). The incident light was aligned perpendicular to the surface of the specimens. The SpectraSuite was used as an operating software for the spectrometer. The spectra changes were monitored by high-speed acquisition mode (Capture period: 0.5 s).

RESULTS AND DISCUSSION

In our recent papers, we have developed a rapid EPD process to form the colloidal crystal film with an EtOH−water colloidal suspension.[24,25] However, the detailed mechanism of the process is still not clear yet. Also, we have observed color change during the drying stage. Thus, in this paper, we have focused on the drying stage after pulling out the ITO/glass substrate from the PS colloidal suspension. Figure 2 shows the SEM images of the colloidal crystal film on the ITO/glass substrate after the EPD and drying processes. Figure 2A shows the top surface of the colloidal crystal film on the substrate. A closely packed PS colloidal hexagonal array was observed for

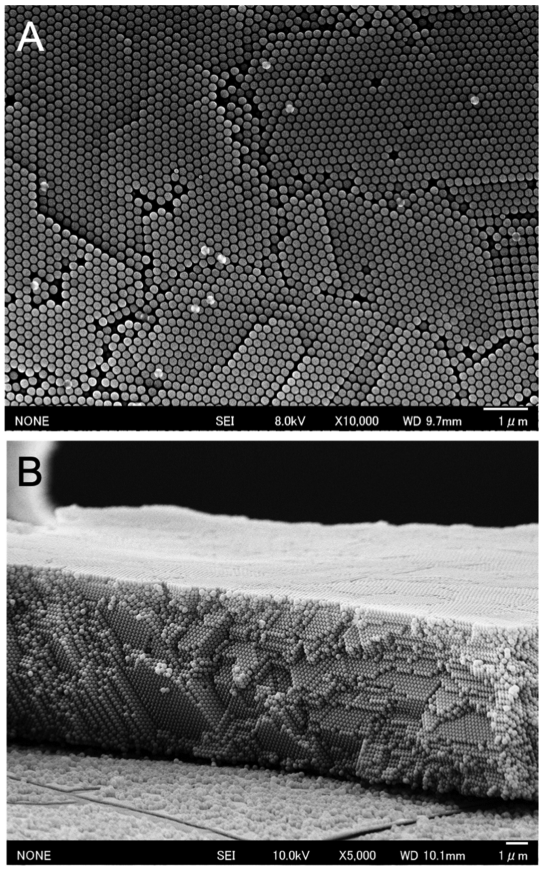

Figure 2. SEM images of the colloidal crystal film: (A) top surface and (B) cross section.

https://dx.doi.org/10.1021/acs.langmuir.0c01048
Langmuir 2020, 36, 10683−10689

almost the whole area, while a very small part of the area was a cubic array. Figure 2B shows the cross-sectional image of the colloidal crystal film edge, which has a blue-green coloring. From the SEM images and our previous study, PS colloidal particles are closely packed and form a face-centered cubic (fcc) lattice with (111) planes aligned to the substrate. This film shows a structural color peak at 498.6 nm due to Bragg's diffraction of the colloidal crystal film. In general, the wavelength of the diffraction peak, λ, of the light diffraction from the colloidal crystal film, i.e., structural color, is expressed by the modified Bragg's diffraction considering the Snell's refraction law as follows[16]

$$\lambda = 2dn_{\mathrm{eff}} = 2d(V_{\mathrm{p}}n_{\mathrm{p}}{}^2 + V_{\mathrm{m}}n_{\mathrm{m}}{}^2)^{1/2} \quad (1)$$

where d, n_{eff}, n_{p}, n_{m}, V_{p}, and V_{m} are the lattice spacings of the arrayed colloids, the effective refractive index of the colloidal crystal, refractive indices of PS particles and the surrounding medium (either air or mixture of ethanol and water), volume fractions of the PS particles and the surrounding medium, respectively. In the case of the fcc lattice, eq 1 becomes as follows since V_{p} and V_{m} are 0.74 and 0.26, respectively

$$\lambda_{\mathrm{cal}} = 2d_{111}(0.74\, n_{\mathrm{p}}{}^2 + 0.26\, n_{\mathrm{m}}{}^2)^{1/2} \quad (2)$$

where $n_{\mathrm{p}} = 1.59$ (PS particle), $n_{\mathrm{m}} = 1$ (air), and $d_{111} = (2/3)^{1/2}D = 166.7$ nm (D is the diameter of the PS particle). From eq 2, the calculated peak diffraction wavelength, λ_{cal}, becomes 486.7 nm. This is almost the same as the measured one, λ_{mes} (498.6 nm).

Figure 3 shows the color change of the colloidal crystal film depending on the elapsed time after pulling out the substrate

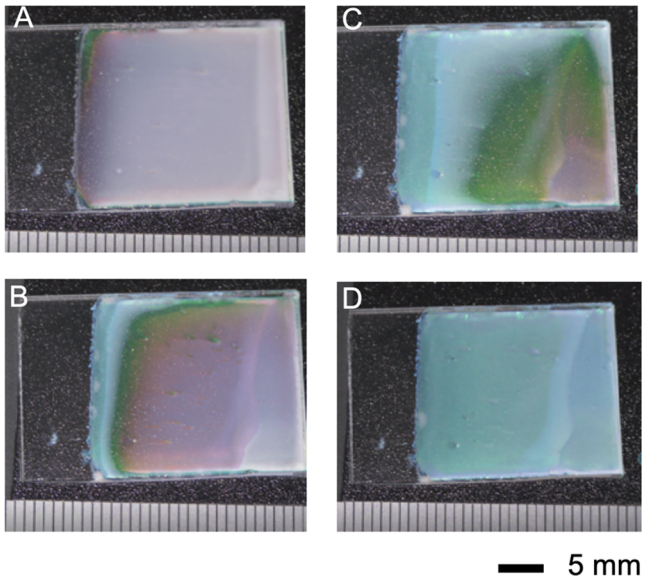

Figure 3. Change from a wet liquid film to the dry colloidal crystal film after pulling out the substrate from the suspension. CCD snapshot images at each elapsed time: (A) 11.5 s, (B) 25 s, (C) 35 s, and (D) 55 s.

from the colloidal suspension. In the beginning, all surfaces of the wet colloidal suspension film showed a milky white color. Then, it turned to the uniform reddish color (Figure 3A). Drying up the solvent proceeded along with the substrate withdrawn direction, i.e., left to right direction of the substrate. This is because the drying process is already accompanied by pulling out the film from the suspension, and the upper suspension liquid film becomes thinner than the lower one on the substrate. By the progress of the drying, the iridescent structural color development was observed, i.e., red, orange, yellow, green, and light blue (Figures 3B,C). Finally, the whole surface of the film was dried up and showed a blue-green color (Figure 3D). The drying up process was completed within 55 s. As described later, the color change in the drying stage was due to the variation of Bragg's diffraction conditions, especially the lattice spacing of the arrayed colloids and the effective refractive index of colloidal crystal film from wet to dry condition. In addition, the color change of the drying process is shown in the Supporting Movie File (Video_S1).

The color change in the drying stage was investigated by the local spectroscopy. After the complete withdrawal of the substrate from the suspension, it took about 10 s until the substrate was fixed at the proper position to measure the reflection spectra. Figure 4 shows the representative reflection

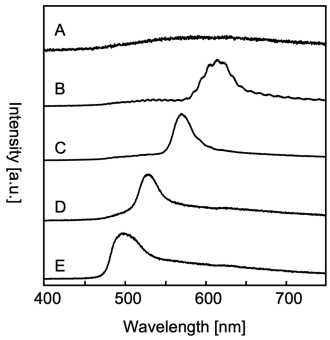

Figure 4. Change in reflection spectra in the drying process by evaporation. The elapsed time was (A) 11 s, (B) 15 s, (C) 27 s, (D) 31 s, and (E) 50 s after pulling out the substrate from the suspension.

spectra measured at the center of the film. After the substrate was removed from the suspension, until 11.0 s (A) the liquid film showed milky and white no reflection peak was observed. At 15.0 s (B), a reflection peak suddenly appeared at around 615.5 nm. This peak corresponded to the red structural color.

The details of the change between spectrum A and B in Figure 4 are shown in Figure 5. At 11.5 s, a small and broad peak was formed around 645.6 nm. The reflection peak at 12.0 s was located around 629.6 nm. The peak position shifted to 615.5 nm at 15.0 s (B).

Since then, at 27 s (C), 31 s (D), and 50 s (E), the reflection peak showed a blue shift continuously over time. The detailed changes of the spectra from B to D and around E are shown in Figures 6 and 7, respectively.

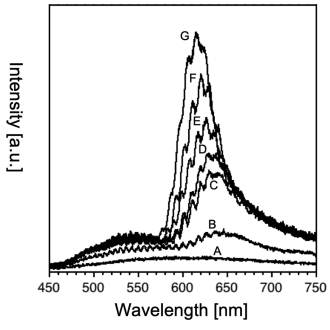

Figure 5. Change of reflection spectra in the drying process by evaporation. The elapsed time was (A) 11 s, (B) 11.5 s, (C) 12 s, (D) 12.5 s, (E) 13 s, (F) 14 s, and (G) 15 s after pulling out the substrate from the suspension.

https://dx.doi.org/10.1021/acs.langmuir.0c01048
Langmuir 2020, 36, 10683−10689

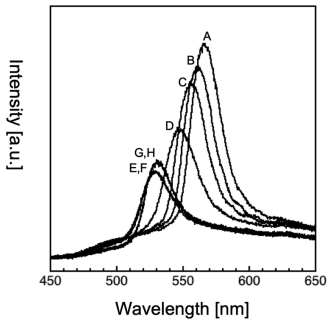

Figure 6. Change in the reflection spectra in the drying process by evaporation. The elapsed time was (A) 27 s, (B) 28 s, (C) 29 s, (D) 30 s, (E) 31 s, (F) 32 s, (G) 33 s, and (H) 34 s after pulling out the substrate from the suspension.

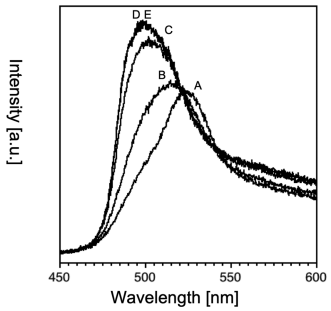

Figure 7. Change of reflection spectra in the drying process by evaporation. The elapsed time was (A) 45 s, (B) 47 s, (C) 49 s, (D) 51 s, and (E) 53 s after pulling out the substrate from the suspension.

Figure 8 shows the change in the reflection peak wavelength depending on the elapsed time after pulling out the substrate

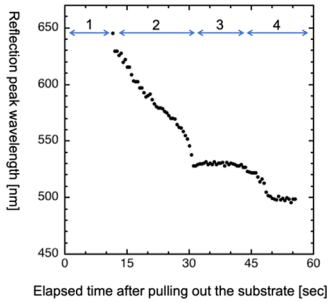

Figure 8. Bragg's diffraction peak position change depending on the elapsed time after pulling out the substrate from the suspension.

from the suspension. From 0 s to just before 11.5 s (defined as range 1), colloidal particles in the aqueous EtOH suspension have a nonordered structure, i.e., random disorder state. And then, at 11.5 s, the reflection peak corresponding to the structural color appeared, i.e., colloidal particles in the concentrated suspension formed the ordered structure caused by Alder's phase transition. A similar phenomenon was reported on the oil covering method to form the high-quality colloidal crystal film.[26] From 11.5 to 31 s (defined as range 2), the blue shift of the reflection peak wavelength continued from 645.6 to 528 nm. The intensity of the diffraction peak increased from 11.5 to 15 s in the first part of range 2, as shown in Figure 5, while it decreased from 27 to 31 s in the second part of range 2, as shown in Figure 6. From 31 to 43 s (defined as range 3), the wavelength of the reflection peak remained almost plateau. From 31 to 34 s shown in Figure 6, diffraction peaks showed stable features, i.e., similar peak position and intensity. Thereafter, from 43 to 60 s (defined as range 4), the blue shift of the reflection peak wavelength took place once again; finally, it kept the constant wavelength of around 500 nm after around 51 s. Figure 7 shows the spectrum change of range 4, the final stage of the drying process. From 45 to 49 s, the diffraction peak wavelength showed a little blue shift from 522 to 502 nm. This second-time reflection peak wavelength change was not observed in the oil covering method.[26]

Furthermore, a morphological change during the drying process of the film with an optical microscope was investigated. Figure 9 shows the optical microscopy photos during the drying

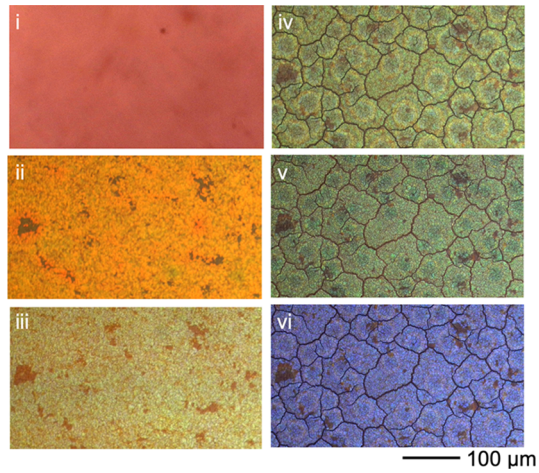

Figure 9. Optical microscopy images during the drying process by evaporation. (i) Milky white colloidal suspension, (ii) structural color (red), (iii) structural color (orange), (iv) cracks formation, (v) wet film (green), and (vi) dry film (blue).

process, from the wet suspension liquid film to the dried colloidal crystal film. The photo (i) shows the colloidal suspension on the substrate before Alder's phase transition. After Alder's phase transition, the structural color was observed as shown in the photo (ii). The color changed from red to orange as shown in the photo (iii). From the photos (i) to (iii), the morphology was almost uniform. After that, between the photo (iii) (elapsed time 15 s) and the photo (iv) (elapsed time: 19 s), many cracks occurred in the colloidal crystal film. Between 31 and 34 s of elapsed time (the photo (v)), there was almost no color change (range 3 of the photo (iv)). After 42 s of elapsed time, the structure color changed from green to blue, and after 52 s of elapsed time (the photo (vi)), the blue color remained constant. This color change from green to blue was caused by drying the wet colloidal crystal film, corresponding to the range 4 of Figure 5. One of the things to be noticed in the optical microscopy imaging is the fact that the multigrain (observed in SEM images as shown in Figure 2) was formed during the early stage of the drying process but not in the last stage. As shown in Figure 6, no crack was formed until 15 s of elapsed time (the photo (iii)). After 15.5 s of elapsed time, a crack was formed until 19 s of elapsed time (the photo (iv)). After that, no more crack formation was observed. This shows that cracks were formed in a very short period for about 4 s, and thereafter crack development stops, i.e., crack formation and development takes place in the middle of the range 2. Thus, the crack formation originated from the nonhomogeneous lattice space reduction of

https://dx.doi.org/10.1021/acs.langmuir.0c01048
Langmuir 2020, 36, 10683−10689

the arrayed colloid film during the range 2. The video of the drying process is shown in Supporting Information Video_S2.

Based on these results, we proposed a model of the colloidal crystal formation accompanied by an evaporating solvent. Figure 10 shows the schematic model of the colloidal crystal film formation categorized into four stages.

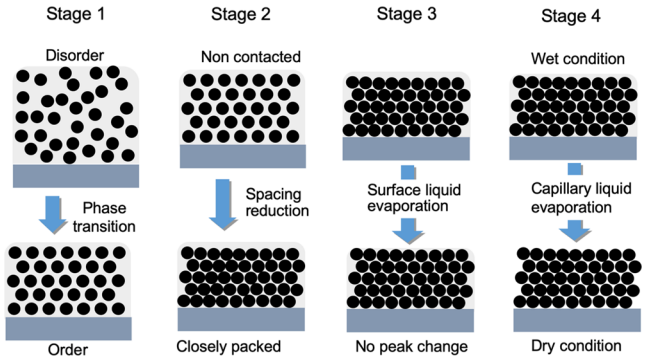

Figure 10. Schematic of the colloidal crystal film formation mechanism after the EPD process and during the drying process.

Stage 1 (disorder-to-order transition): After the electrophoresis, the surface of the ITO/Glass is covered with a colloidal suspension containing PS particles as a liquid film composed of a mixture of EtOH and water. In this period, PS particles are dispersed in the liquid with Brownian random motion. No specific reflection peak is observed so that the color of the film looks milky white. With the progress of suspension drying, a self-assembled nonclosely packed PS colloidal crystal film is formed due to the phase transition from the disorder-to-order state, i.e., disorder-to-order Alder's phase transition (between Figure 5A,B). This causes the color of the film to change from milky white to red (corresponding to the range 1 of Figure 8). In addition, we recognize this color change from the movie of the optical microscope. Around 10−11 s, the phase transition of colloidal crystallization suddenly occurred, and the color changed quickly.

Stage 2 (tuning the lattice distance and changing the colloidal crystal from noncontact to contact): The evaporation of aqueous EtOH solvent from the wet film of colloidal suspension continues. At the same time, the lattice spacing and the interparticle distance, d, shrinks continuously. Finally, colloidal crystal reaches a dense closely packed structure. At this stage, a lattice spacing, d, plays an important role in the peak shift. This process causes the shift in the reflection peak wavelength from red to green color (the range 2 of Figure 8). In addition, crack formation is involved in this stage due to the volume shrinking of the colloidal crystal film from the observation of the optical microscope.

Stage 3 (evaporating surface liquid on the colloidal crystal film): After forming a closely packed structure, the PS particle layer was covered with a liquid film of aqueous EtOH. The reflection peak shows s constant wavelength at green color because the d value almost does not decrease (the range 3 of Figure 8), i.e., shrinking of lattice spacing, d, almost stops. Bragg's diffraction is caused only by the particle layers. During the evaporation, we observed tentatively the iridescence color shown in the photo (iv) in Figure 9. The iridescence is due to the thin-film interference of the surface liquid over the colloidal crystal.

Stage 4 (liquid evaporation from the interparticle spacing of the colloidal crystal film): Evaporation of interparticle liquid, i.e., capillary liquid, takes place. This leads to the change of n_{eff} due to the exchange of interparticle medium from the liquid to air. Consequently, the reflection peak wavelength shifts from green to blue color and realizes the dry closely packed colloidal crystal structure (the range 4 of Figure 8). At this stage, the change of the refractive index becomes an important parameter to determine Bragg's diffraction peak. During stage 4, the peak shift was 20 nm (from 522 to 502 nm). The effective refractive index can be calculated as follows: from eq 2, $n_{eff} = (0.74\ n_p^2 + 0.26\ n_m^2)^{1/2}$. Here, we used $n_p = 1.59$, $n_m = 1$ (Dry) or 1.36 (wet, EtOH). We can obtain the change in n_{eff} from 1.53 to 1.46. The diffraction peak position is reduced by 95.4%. This reduction rate is reasonable, 522 nm/502 nm (96.2%). However, it is not a clear change of d_{111} planes during stage 4.

The above crystallization mechanism is basically a similar process based on Alder's phase transition in the colloidal process due to the concentrating colloidal suspension.[26−31] In the case of the oil covering method,[26] the colloidal crystal film is formed under the silicone oil layer in stage 1 (Phase transition) and stage 2 (Spacing reduction). The crystal growth rate was very slow. A few days were required to form a colloidal crystal film on a 4 in. silicon substrate. In contrast, the crystal growth rate in this work was 0.5 mm/s. These results suggest that the growth rate is about 1000 times faster if we do not consider the quality of colloidal crystal films. In the case of the evaporative self-assembly process, Koh et al. have reported a similar model using a vertical and horizontal colloidal deposition process.[27,28] In the model and reflectance spectra, they proposed a crystallization process as the following three steps, i.e., phase transition, decreasing lattice space, and dry up. In this work, there are the corresponding similar model stage 1, stage 2, and stage 4, respectively. However, stage 3 in our model is a little different from the previous similar drying processes.[27,28]

At this time, the phenomenon (the reflection peak of the plateau in region 3 in Figure 8) is tentatively explained in our stage 3 model. We are interested in a similar phenomenon reported by the previous works. Marlow et al. investigated in detail the mechanism of capillary deposition.[29,30] They have reported an in situ observation of wet opal formation from a dilute colloidal suspension by spectroscopy. They conclude that there are three specific internal changes in wet opal films: crystallization, compression, and defect formation.[30] They also previously reported the drying of the colloidal crystals process and strange red shift due to the transformation of water from shells to a neck-type distribution (v-event).[29] In their process (Capillary deposition), Bragg's diffraction peak shift is a slow process lasting a few hours. Meng et al. have reported on colloidal crystal formation by evaporation-induced self-assembly using CCD camera and spectroscopy.[31] From their paper, the entire drying process contains three stages: crack-initiation stage, crack-propagation stage, and crack-remaining stage. They found a red shift of Bragg's diffraction when crack begins to propagate in the crack-propagation stage. At this time, the phenomenon has not been completely explained in our Stage 3 model, and further detailed analysis is needed in the future.

https://dx.doi.org/10.1021/acs.langmuir.0c01048
Langmuir 2020, 36, 10683−10689

However, the peak shift time is completed within 1 min. This colloidal crystallization is an extremely rapid process compared with previous reports.[26−31]

CONCLUSIONS

A growth mechanism of the colloidal crystal films from the concentrated aqueous EtOH suspension has been investigated. Closely packed colloidal crystal film was formed within 55 s. By the analysis of the reflection spectra and the optical microscopy images, the growth mechanism from the colloidal suspension to the colloidal crystal film was found to consist of four stages. The first stage is a liquid film of the concentrated colloidal suspension on a substrate. With the progress of evaporation, the phase transition from disorder to order to form a nonclosely packed colloidal crystal by self-assembly takes place. At the time of the phase transition, the Bragg's diffraction peak is detected and the structural color appears. In the second stage, the diffraction peak shifts toward the shorter-wavelength direction (blue shift) due to the reduction of the interparticle distance of the nonclosely packed colloidal crystal. In the end, the closely packed colloidal crystal film is formed. In the third stage, the liquid film covering the colloidal crystal film evaporated and iridescence color due to thin-film interference is tentatively observed. In the fourth stage, the colloidal crystal film changes from wet to dry by the evaporation of the interparticle aqueous EtOH solvent. The structural color changes from green to blue and the diffraction peak wavelength goes down with one more stage. This color change is dominated by the change of the refractive index of the interparticle medium from the liquid to the air. One of the key findings in our process is rapid crystal growth using concentrated colloid EtOH suspension. The growth speed of the colloidal crystal is extremely rapid (within 1 min for 900 mm^2 area) compared with those of previous papers, such as oil covering and capillary deposition methods (several to hundreds of hours). This process has the potential for high-speed deposition of the colloidal crystalline thin films.

ASSOCIATED CONTENT

Supporting Information

The Supporting Information is available free of charge at https://pubs.acs.org/doi/10.1021/acs.langmuir.0c01048.

The video files clearly show the dynamic change in color and morphology from suspension to colloidal crystal films (PDF)

Video_S1: Drying process of the concentrated polystyrene colloidal suspension film observed with a digital 4K video camera. The snapshot photos in Figure 3 are taken from this video file (MP4)

Video_S2: Color and morphology changed during evaporation under the observation of an optical microscope. The movie was recorded using a high-resolution CMOS camera. The snapshot photos from the movie are shown in Figure 9 (MP4)

AUTHOR INFORMATION

Corresponding Author

Hiroshi Fudouzi − *National Institute for Materials Science, Tsukuba, Ibaraki 305-0047, Japan;* orcid.org/0000-0003-1442-4667; Phone: +81-29-859-2450; Email: FUDOUZI.Hiroshi@nims.go.jp

Authors

Giang T.H. Tran − *National Institute for Materials Science, Tsukuba, Ibaraki 305-0047, Japan; Graduate School of Engineering, Hokkaido University, Sapporo, Hokkaido 060-0808, Japan*

Masaki Koike − *National Institute for Materials Science, Tsukuba, Ibaraki 305-0047, Japan*

Tetsuo Uchikoshi − *National Institute for Materials Science, Tsukuba, Ibaraki 305-0047, Japan; Graduate School of Engineering, Hokkaido University, Sapporo, Hokkaido 060-0808, Japan;* orcid.org/0000-0003-3847-4781

Complete contact information is available at: https://pubs.acs.org/10.1021/acs.langmuir.0c01048

Notes

The authors declare no competing financial interest.

ACKNOWLEDGMENTS

The part of this work was supported by KAKENHI Grant-in-Aid for Scientific Research (B: #20H02510). One of the authors, T.U., was financially supported by the JST A-Step program, Grant Number JPMJTS1615, Japan.

REFERENCES

(1) Arsenault, A. C.; Miguez, H.; Kitaev, V.; Ozin, G. A.; Manners, I. A Polychromic, Fast Response Metallopolymer Gel Photonic Crystal with Solvent and Redox Tunability: A Step Towards Photonic Ink (P-Ink). *Adv. Mater.* **2003**, *15*, 503−507.

(2) Fudouzi, H.; Xia, Y. N. Photonic Papers and Inks: Color Writing with Colorless Materials. *Adv. Mater.* **2003**, *15*, 892−896.

(3) Zhang, J.; Li, Y.; Zhang, X.; Yang, B. Colloidal Self-Assembly Meets Nanofabrication: from Two-Dimensional Colloidal Crystals to Nanostructure Arrays. *Adv. Mater.* **2010**, *22*, 4249−4269.

(4) Zhang, T.; Ma, Y.; Qi, L. Bioinspired Colloidal Materials with Special Optical, Mechanical, and Cell-Mimetic Functions. *J. Mater. Chem. B* **2013**, *1*, 251−264.

(5) Cong, H.; Yu, B.; Tang, J.; Li, Z.; Liu, X. Current Status and Future Developments in Preparation and Application of Colloidal Crystals. *Chem. Soc. Rev.* **2013**, *42*, 7774−7800.

(6) Stein, A.; Wilson, B. E.; Rudisill, S. G. Design and Functionality of Colloidal-Crystal-Templated Materials-Chemical Applications of Inverse Opals. *Chem. Soc. Rev.* **2013**, *42*, 2763−2803.

(7) Vogel, N.; Retsch, M.; Fustin, C. A.; Campo, A. D.; Jonas, U. Advances in Colloidal Assembly: the Design of Structure and Hierarchy in Two and Three Dimensions. *Chem. Rev.* **2015**, *115*, 6265−6311.

(8) Lai, C. F.; Wang, Y. C. Colloidal Photonic Crystals Containing Silver Nanoparticles with Tunable Structural Colors. *Crystals* **2016**, *6*, No. 61.

(9) Dimitrov, A. S.; Nagayama, K. Continuous Convective Assembling of Fine Particles into Two-Dimensional Arrays on Solid Surfaces. *Langmuir* **1996**, *12*, 1303−1311.

(10) Rakers, S.; Chi, L. F.; Fuchs, H. Influence of the Evaporation Rate on the Packing Order of Polydisperse Latex Monofilms. *Langmuir* **1997**, *13*, 7121−7124.

(11) van Blaaderen, A.; Ruel, R.; Wiltzius, P. Template-Directed Colloidal Crystallization. *Nature* **1997**, *385*, 321−324.

(12) Mayoral, R.; Requena, J.; Moya, J. S.; López, C.; Cintas, A.; Miguez, H.; Meseguer, F.; Vázquez, L.; Holgado, M.; Blanco, A. 3D Long-Range Ordering in ein SiO_2 Submicrometer-Sphere Sintered Superstructure. *Adv. Mater.* **1997**, *9*, 257−260.

(13) Jiang, P.; Bertone, J. F.; Hwang, K. S.; Colvin, V. L. Single-Crystal Colloidal Multilayers of Controlled Thickness. *Chem. Mater.* **1999**, *11*, 2132−2140.

(14) Gu, Z. Z.; Fujishima, A.; Sato, O. Fabrication of High-Quality Opal Films with Controllable Thickness. *Chem. Mater.* **2002**, *14*, 760−765.

(15) Gates, B.; Xia, Y. Fabrication and Characterization of Chirped 3D Photonic Crystals. *Adv. Mater.* **2000**, *12*, 1329−1332.
(16) Fudouzi, H. Fabricating High-Quality Opal Films with Uniform Structure over a Large Area. *J. Colloid Interface Sci.* **2004**, *275*, 277−283.
(17) Fu, Y.; Jin, Z.; Liu, G.; Yin, Y. Self-assembly of polystyrene sphere colloidal crystals by in situ solvent evaporation method. *Synth. Met.* **2009**, *159*, 1744−1750.
(18) Kleinert, J.; Kim, S.; Velev, O. D. Electric-Field-Assisted Convective Assembly of Colloidal Crystal Coatings. *Langmuir* **2010**, *26*, 10380−10385.
(19) Kanai, T.; Sawada, T.; Toyotama, A.; Kitamura, K. Air-Pulse-Drive Fabrication of Photonic Crystal Films of Colloids with High Spectral Quality. *Adv. Funct. Mater.* **2005**, *15*, 25−29.
(20) Rogach, A. L.; Kotov, N. A.; Koktysh, D. S.; Ostrander, J. W.; Rgaisha, G. A. Electrophoretic Deposition of Latex-Based 3D Colloidal Photonic Crystals: A Technique for Rapid Production of High-Quality Opals. *Chem. Mater.* **2000**, *12*, 2721−2726.
(21) Huang, Y. J.; Lai, C. H.; Wu, P. W. Fabrication of Large-Area Colloidal Crystals by Electrophoretic Deposition in Vertical Arrangement. *Electrochem. Solid-State Lett.* **2008**, *11*, P20−P22.
(22) Katagiri, K.; Tanaka, Y.; Uemura, K.; Inumaru, K.; Seki, T.; Takeoka, Y. Structural Color Coating Films Composed of an Amorphous Array of Colloidal Particles via Electrophoretic Deposition. *NPG Asia Mater.* **2017**, *9*, No. e355.
(23) Lai, C. H.; Huang, Y. J.; Wu, P. W.; Chen, L. Y. Rapid Fabrication of Cylindrical Colloidal Crystals and Their Inverse Opals. *J. Electrochem. Soc.* **2010**, *157*, P23−P27.
(24) Koike, M.; Tran, G. T. H.; Azuma, S.; Kiyono, H.; Uchikoshi, T.; Fudouzi, H. Rapid fabrication of colloidal crystal films by electrophoretic deposition and its application for a volatile liquid and strain detection sensor. *J. Soc. Powder Technol., Jpn.* **2019**, *56*, 339−346.
(25) Tran, G. T. H.; Koike, M.; Uchikoshi, T.; Fudouzi, H. Fabrication of polystyrene colloidal crystal film by electrophoretic deposition. *Adv. Powder Technol.* **2020**, *31*, 3085−3092.
(26) Fudouzi, H. Novel Coating Method for Artificial Opal Films and its Process Analysis. *Colloids Surf., A* **2007**, *311*, 11−15.
(27) Koh, Y. K.; Wong, C. C. In Situ Monitoring of Structural Changes During Colloidal Self-assembly. *Langmuir* **2006**, *22*, 897−900.
(28) Koh, Y. K.; Yip, C. H.; Chiang, Y. M.; Wong, C. C. Kinetic Stages of Single-Component Colloidal Crystallization. *Langmuir* **2008**, *24*, 5245−5248.
(29) Muldarisnur, M.; Marlow, F. Spectroscopic Investigation of Opal Formation from Suspensions. *J. Phys. Chem. C* **2017**, *121*, 18274−18279.
(30) Muldarisnur, M.; Marlow, F. Observation of Nano-Dewetting in Colloidal Crystal Drying. *Angew. Chem., Int. Ed.* **2014**, *53*, 8761−8764.
(31) Lin, D.; Wang, L.; Yang, L.; Luo, Y.; Li, D.; Meng, Q. Real-Time Synchronous CCD Camera Observation and Reflectance Measurement of Evaporation-Induced Polystyrene Colloidal Self-Assembly. *Langmuir* **2014**, *30*, 3949−3956.

https://dx.doi.org/10.1021/acs.langmuir.0c01048
Langmuir 2020, 36, 10683−10689